RESEARCH ARTICLE

Dynamical properties of water in living cells

Irina Piazza[1,2,†], **Antonio Cupane**[1], **Emmanuel L. Barbier**[3,4], **Claire Rome**[3,4], **Nora Collomb**[3,4],
Jacques Ollivier[2], **Miguel A. Gonzalez**[2], **Francesca Natali**[5,2,‡]

[1] *Dept. of Physics and Chemistry, University of Palermo, Viale delle Scienze Ed. 18, 90122 Palermo, Italy*
[2] *Institut Laue-Langevin, 71 avenue des Martyrs, 38042 Grenoble Cedex 9, France*
[3] *Institut des Neurosciences, Université Grenoble-Alpes, 38044 Grenoble, France*
[4] *Inserm, U1216, Grenoble, France*
[5] *CNR-IOM, OGG, 6 rue Jules Horowitz, 38042 Grenoble Cedex 9, France*
Corresponding authors. E-mail: †piazzai@ill.fr, ‡natali@ill.fr
Received April 10, 2017; accepted July 12, 2017

With the aim of studying the effect of water dynamics on the properties of biological systems, in this paper, we present a quasi-elastic neutron scattering study on three different types of living cells, differing both in their morphological and tumor properties. The measured scattering signal, which essentially originates from hydrogen atoms present in the investigated systems, has been analyzed using a global fitting strategy using an optimized theoretical model that considers various classes of hydrogen atoms and allows disentangling diffusive and rotational motions. The approach has been carefully validated by checking the reliability of the calculation of parameters and their 99% confidence intervals. We demonstrate that quasi-elastic neutron scattering is a suitable experimental technique to characterize the dynamics of intracellular water in the angstrom/picosecond space/time scale and to investigate the effect of water dynamics on cellular biodiversity.

Keywords quasi-elastic neutron scattering, intracellular water, water structure and dynamics

PACS numbers 83.86.Hg, 87.16.dg, 61.05.fg

Frontiers of Physics

1 Introduction

The relevance of water structure and dynamics in biological systems is widely recognized in the scientific literature [1]. As far as neutron scattering experiments are concerned, evidence of the essential role of water originates from polypeptides and protein powders, where the activation of functionally relevant motions (the so-called protein dynamical transition –PDT) has been related to the physical properties (structure and dynamics) of hydration water [2, 3], up to intact cells, where the presence of water reaching up to 80% of the total weight is required to preserve their function [4, 5]. Water dynamics in intact cells has been the subject of extensive investigations using quasi-elastic neutron scattering (QENS) and nuclear magnetic resonance (NMR), for more than 30 years [6]. However, no consensus about water diffusion coefficient(s) inside cells has been reached

yet [1], while apparently contradicting results have been reported, giving rise to intensive debates in the literature. In fact, QENS studies on E. coli [7, 8] and red blood cells [9] showed that the short-range (subnanometer scale) translational dynamics of the majority of intracellular water is essentially unaltered with respect to bulk water, while only a small fraction has a dynamics slower by one order of magnitude. Conversely, in the case of Haloarcula marismortui (Hmm; an extremely thermophilic bacterium), both the fraction of slow water molecules and the extent of slowing down was found to increase dramatically. Interestingly, NMR studies of water rotational dynamics in the same cells [10] reported very similar results for E. coli and Hmm, i.e., a majority of intracellular water with bulk-like rotational dynamics and only a small fraction with one order of magnitude slower dynamics. This points out the necessity of further investigations where the effects of cellular biodiversity are taken into account, and the different types of motions are properly disentangled. In this paper we present a QENS study on water dynamics in three widely different living cells (E. coli, yeast Schizosaccharomyces

pombe cells, and rat Glioma-9L tumoral cells). The aim of the work is to study the effects of biodiversity by applying an optimized theoretical model that allows disentangling various types of motions to the analysis of QENS data. A particular emphasis is placed on the validation of the model and on the careful verification of the reliability of the results obtained by the fitting procedure.

2 Materials and methods

2.1 Samples

Cells used for the experiments were:

- Escherichia coli strain BL21(DE3)pLysS (Promega, Fitchburg, WI, USA). Cells colonies were grown on Luria-Bertani Agar medium plate at 37°C overnight. One colony was dissolved in 250 mL of Luria-Bertani medium and let to grow overnight at 37°C under gentle stirring (250 rpm).
- Rat Glioma-9L cells (American Type Culture Collection, Manassas, VA); CRL-2200, were grown in Roswell Park Memorial Institute medium (RPMI) 1640 supplemented with 10% FBS and (100 units/ml) streptomycin (100 µg/ml). Cells were grown in tissue culture dishes in a humidified incubator (37°C, 5% CO_2) and were passaged when they were nearly confluent.
- Yeast Schizosaccharomyces pombe cells were grown with standard procedures for vegetative in Edinburgh Minimal Medium [11].

The cell cultures were kept at 4°C in PBS buffer pH=7.4 to guarantee physiological conditions and to prevent cell death. Immediately before the experiments, they were centrifuged for 7 min at 7000 rpm, the supernatant was discarded and the remaining pellet used for experiments. The hydration of samples was measured at the end of the neutron scattering experiments by drying and weighting. E. coli, yeast, and Glioma-9L contained water at 64%, 69%, and 50% by weight, respectively. In pellets of E. coli it has been reported that approximately 90% of the water present is intracellular and only less than 10% is extracellular [12]. Although small variations, in the order of a few percent, may be present for the other cell pellets, it can be safely assumed that in our samples most of the water is intracellular. Images of the samples were taken with optical zoom 100×, before and after the experiment, using a standard fluorescence microscope at EMBL (Grenoble, France), in order to check that the cells were still alive and without any degradation effect. Trypan blue exclusion tests, which allow distinguishing dead cells from
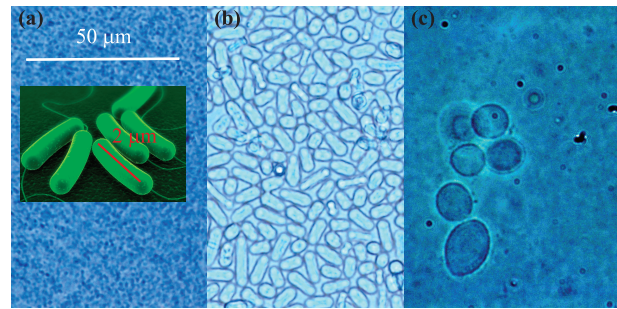
Fig. 1 Sample image taken before the experiment by fluorescence microscope. **(a)** E. coli cells. **(b)** Yeast Schizosaccharomyces pombe cells. **(c)** Glioma-9L cells.

alive ones, were also executed and viability of the cells was ensured until the end of the experiments. As can be seen in Fig. 1, E. coli are rod-shaped bacteria, which are about 2.0 µm long and 0.25 µm in diameter, with a cell volume of 0.6 µm^3; yeast cells (eukaryotic microorganisms classified in the kingdom Fungi), are also roughly rod-shaped, typically measuring 5–10 µm in length and 1–2 µm in diameter; Glioma-9L are almost spherical (diameter of about 10 µm) tumor cells obtained in vitro and very useful for *in vivo* studies to investigate the effects of various therapeutic agents on brain tumors.

2.2 QENS experiments

Quasi-elastic neutron scattering experiments were performed by using the high-resolution direct-geometry time-of-flight (TOF) spectrometer IN5 at the Institut Laue-Langevin (ILL, Grenoble, France). The samples were placed in a vacuum-tight aluminum rectangular sample holder with thickness of 0.3 mm and area of 30×40 mm^2. In order to properly explore translational and rotational components in the spectra, the experiments were performed at two different energy resolutions: 10 µeV full width at half maximum (FWHM), corresponding to a time resolution of ~ 70 ps and Q-range between 0.11 and 1.01 Å^{-1}, and 70 µeV FWHM, corresponding to a time resolution of ~ 10 ps and Q-range between 0.22 and 2.02 Å^{-1}. All measurements were conducted at room temperature (300 K). All measured spectra were corrected for the empty cell contribution and normalized to vanadium. Spectra measured at Q values lower than 0.3 Å^{-1} were rejected as they were affected by Bragg peaks due to cellular membranes, as observed in the diffraction pattern (data not shown). 26 spectra were analyzed in global fittings (see below): 12 at high-energy resolution and 14 at low-energy resolution. The STRfit tools in the LAMP software, developed by the computing group at ILL [13] were used for data reduction and analysis.

2.3 Data analysis

The analysis of the QENS spectra measured from our living cells was motivated by several biophysical arguments. First, given the large incoherent scattering cross section, in our samples, the signal arises essentially from hydrogen atoms. We identified several hydrogen classes:

- hydrogen atoms that in the time scale investigated by our experiments ($10 \div 100$ ps) appear as "fixed", i.e., they perform only vibrational motions around their equilibrium positions. We indicate their population fraction with parameter f; their contribution to the scattering signal is purely elastic.

- hydrogen atoms belonging to water molecules with deeply constrained dynamics and slowed down by the interaction with the crowded cellular environment. We indicate their population fraction with parameter p_1; we use the "jump-diffusion" model to describe translations, and the "continuous rotational diffusion on a circle" model to describe rotations [14, 15].

- hydrogen atoms belonging to water molecules, whose dynamics is only weakly constrained by the other cellular components and can, therefore, be considered as freely translating and rotating. We indicate their population fraction with parameter p_2; also for these hydrogens, following an approach commonly used for bulk water [16], we use the "jump diffusion" model for translations and the "rotational diffusion on a circle" model for rotations [15].

- hydrogen atoms belonging to CH_2 groups present in the cell membrane and in cellular proteins; these hydrogen atoms perform low-frequency librational motion at room temperature. We indicate their population fraction with parameter p_3; it follows from the closure relation that $p_3 = 1 - (f + p_1 + p_2)$.

Therefore, the following expression was used to fit the measured spectra:

$$S_{inc}(Q, \omega') = K(Q)R(Q, \omega') \otimes [f\delta(\omega') + p_1 S_{slow}^{R,T}(Q, \omega') + p_2 S_{fast}^{R,T}(Q, \omega') + p_3 S_{CH_2}(Q, \omega')] + bk(Q), \quad (1)$$

where $K(Q)$ is a normalizing factor that includes the Q-dependent Debye–Waller factor and $\omega' = \omega - C(Q)$. Parameters $C(Q)$ were necessary to consider small offsets in the energy calibration of the detectors, thus, parameters $C(Q)$ are the same for all spectral contributions. $R(Q, \omega')$ is the instrumental resolution, measured by a standard vanadium. $\delta(\omega')$ is the Dirac delta function. $S_{slow}^{R,T}(Q, \omega') = S_{slow}^{T}(Q, \omega') \otimes S_{slow}^{R}(Q, \omega')$ is the contribution of constrained water molecules; it contains the convolution of two terms arising from translation and

rotation, respectively, and depends on the parameters D_{slow}^{T}, D_{slow}^{R}, and τ_{slow} that are the translational and rotational diffusion coefficients, and the translational residence time, respectively. According to the models used, the translational and rotational components described by the following expressions:

$$S_{slow}^{T}(Q, \omega') = \frac{1}{\pi} \frac{\Gamma_{slow}^{T}}{(\omega')^2 + (\Gamma_{slow}^{T})^2}, \quad (2)$$

where

$$\Gamma_{slow}^{T} = \frac{Q^2 D_{slow}^{T}}{1 + Q^2 D_{slow}^{T} \tau_{slow}}, \quad (3)$$

and

$$S_{slow}^{R}(Q, \omega') = j_0^2(Qr)\delta(\omega') + \sum_{i=1}^{\infty} (2i+1)j_i^2(Qr)\frac{1}{\pi} \frac{\Gamma_{slow}^{i,R}}{(\omega')^2 + (\Gamma_{slow}^{i,R})^2}, \quad (4)$$

where

$$\Gamma_{slow}^{i,R} = i(i+1)D_{slow}^{R}. \quad (5)$$

Functions $j_i(Qr)$ appearing in the rotational part of $S_{slow}^{R}(Q)$ are spherical Bessel functions of ith order, while quantity r is the average radius of the water hydrogens rotational circles: this quantity was assumed to have a fixed value of 0.98 Å. In the sum in Eq. (4), the first 10 terms were retained. $S_{fast}^{R,T}(Q, \omega) = S_{fast}^{T}(Q, \omega) \otimes S_{fast}^{R}(Q, \omega)$ is the contribution of "free" water molecules. Regarding $S_{slow}^{R,T}(Q)$, it contains the convolution of translations and rotations, and depends on the parameters D_{fast}^{T}, D_{fast}^{R}, and τ_{fast}; the considerations previously made for $S_{slow}^{R,T}(Q)$ apply to $S_{fast}^{R,T}(Q)$ as well. $S_{CH_2}(Q, \omega)$ is the contribution of hydrogens belonging to CH_2 groups located mainly in the cellular membranes; it arises from low-frequency librations and can be modeled by a simple Lorentzian with a Q-independent half-width described by parameter Γ_{CH_2}. $bk(Q)$ is a flat, Q-dependent background, which is necessary to consider the instrumental baseline and other possible much broader contributions. In our data analysis we adopted a "global fitting" strategy, i.e., all spectra obtained at the various Q values and at the two resolutions were analyzed simultaneously, thus greatly reducing the complexity of the χ^2 hypersurface. In the fittings quantities f, p_1, p_2, D_{slow}^{T}, D_{slow}^{R}, τ_{slow}, D_{fast}^{T}, D_{fast}^{R}, τ_{fast}, and Γ_{CH_2} are global parameters, while quantities $K(Q)$, $C(Q)$, and $bk(Q)$ are different for each spectrum. A typical spectrum is shown in Fig. 2 together with the fitting. For the sake of clarity, the spectral contributions arising from various hydrogen

Irina Piazza, et al., Front. Phys. 13(1), 138301 (2018)

138301-3
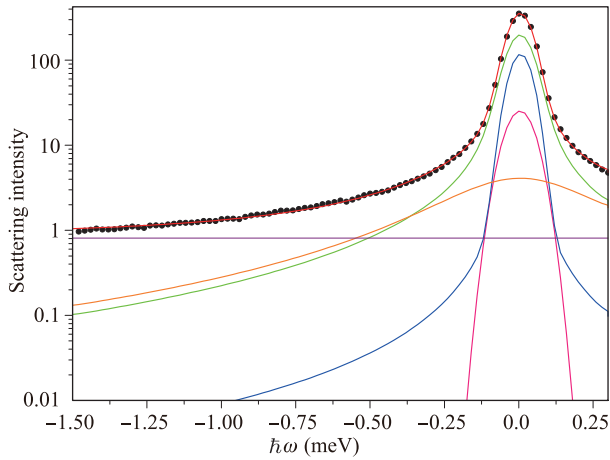
Fig. 2 QENS spectrum of yeast cells taken at 0.36 Å^{-1} at low-energy resolution. Black points are the experimental data and the red line is the total fit obtained using Eq. (1). The various spectral contributions are represented by the lines in color. Fuchsia: elastic contribution arising from "fixed" hydrogen atoms; green: roto-translational contribution arising from "fast" water population; blue: roto-translational component arising from "slow" water population; orange: CH_2 groups contribution; violet: background.

classes are highlighted in the figure. Considering the rather large number of parameters involved in the fittings it was necessary to perform a check on the reliability of their calculation. In particular we analyzed the χ^2 hypersurface by calculating the $\chi^2_{p_i} - \chi^2_{min}$ profile with respect to each global parameter p_i. In these fittings the global parameters different from p_i were kept constant at their χ^2_{min} values, while the non-global parameters can be varied. We repeated the procedure by using two different minimization routines based on the Levenberg-

Marquardt method and implement in the SRTfit by the computing group at ILL [13], in order to further check the robustness of our results. A typical result is shown in panel (a) of Fig. 3 for parameter D^T_{fast}; similar results are obtained for the other parameters as well. This plot shows that single sharp minima are obtained with both minimization routines and illustrates how the 99% confidence limit was determined [17]. Panels (b) and (c) of Fig. 3 show the confidence limit analysis of parameters p_1 and p_2 for the three cell types investigated; they show that our experiments can indeed effectively detect the effects of cellular biodiversity. χ^2 is defined as

$$\chi^2(\boldsymbol{p}) = \sum_{i=1}^{N} \left[\frac{y_i - y(x_i|\boldsymbol{p})}{\sigma_i} \right]^2, \qquad (6)$$

where N is the number of points, y_i are the data points with σ_i errors, $\boldsymbol{p}$ is the vector of parameters, and $y(x_i|\boldsymbol{p})$ is the theoretical model. The validity of the model used was further checked by analyzing QENS data obtained with "phantoms" consisting of water/sugar mixtures at different ratios and with vegetable and animal tissues (data not shown). Results indicated that our model is able to characterize the behavior of water in biological systems of different complexity in a consistent way.

3 Results and discussion

QENS spectra of our samples are shown in Fig. 4. The data in this figure confirm that good fits are obtained using the global model reported in Section 2. Even the simple visual inspection suggests that the QENS spectra are influenced by cellular biodiversity. In fact, spectra corresponding to Glioma-9L cells are broader than those
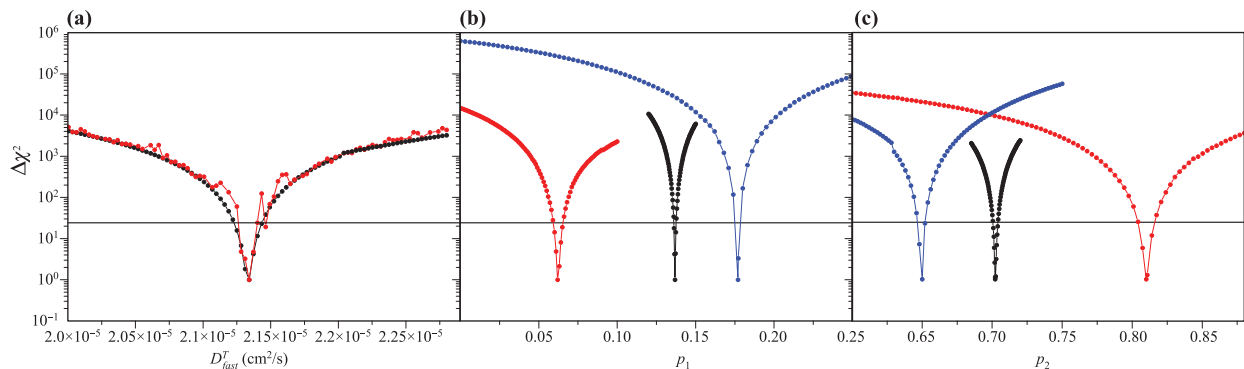
Fig. 3 Panel **(a)**: Confidence limits analysis: $\Delta\chi^2 = \chi^2_{p_i} - \chi^2_{min} + 1$ as a function of parameter D^T_{fast} for the data corresponding to E. coli cells. Red and black dots refer to results obtained with two different minimization routines developed at ILL. The horizontal black line cuts the plot at $\Delta\chi^2 = 24.2$ and determines the 99% confidence intervals. Panel **(b)**: Confidence limits analysis for the for the "slow" water component (parameter p_1). Data corresponding to E. coli, Glioma-9L, and yeast cells are shown in black, red, and blue, respectively. Panel **(c)**: Same as panel (b) for the "fast" water component (parameter p_2).
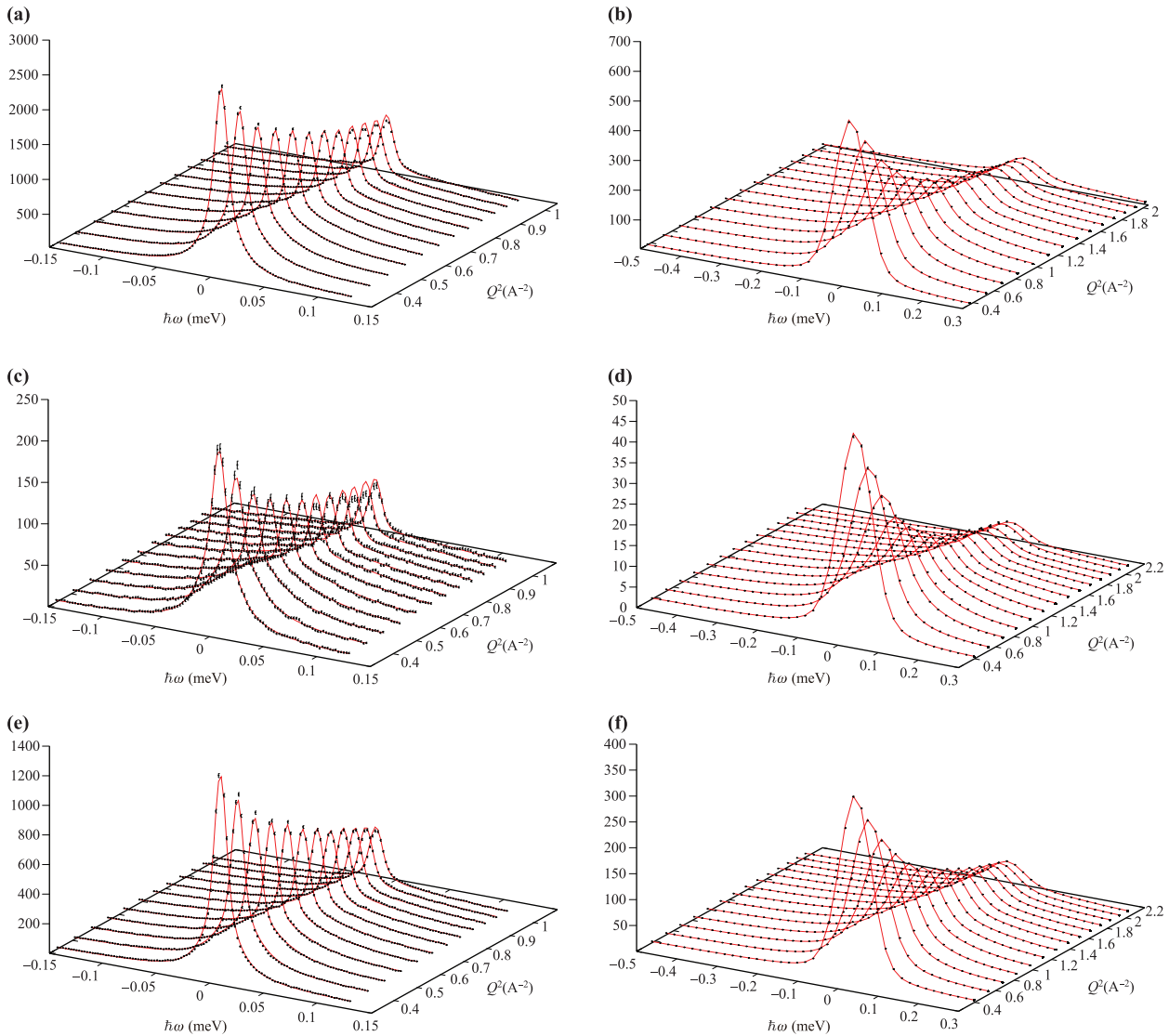
Fig. 4 Left panels: QENS spectra taken at 10 μeV energy resolution; **(a)** E. coli, **(c)** Glioma-9L, **(e)** Yeast. Right panels: QENS spectra taken at 70 μeV energy resolution; **(b)** E. coli, **(d)** Glioma-9L, **(f)** Yeast. Black points (●) are the experimental data and the red lines are the fitting curves.

corresponding to E. coli cells, and decay with increasing Q appreciably faster; differences between the E. coli and yeast spectra are less noticeable. The faster Q-decay observed for Glioma-9L cells may be indicative of a larger Debye–Waller factor, i.e., of larger mean square displacements; elastic neutron scattering (ENS) experiments are currently planned to confirm this suggestion. More quantitative information is obtained from the parameter values obtained from the global fits, summarized in Table 1. The most important finding is that the population of "fast" water molecules accounts for the majority of the scattering signal (from 65% to 80%, depending on the cell type) and characterized by translational and rotational diffusion coefficients very similar to those

of bulk water at room temperature [14] ($D_{bulkwater}^{T} = 2.3 \div 2.5 \cdot 10^{-5}$ cm²/s; $D_{bulkwater}^{R} = 0.17$ ps⁻¹). A possible increase of the residence times of "fast" water with respect to bulk water in the case of E. coli and yeast cells cannot be excluded ($\tau_{bulkwater} = 0.9 \div 1.2$ ps). Such an increase has been previously observed for water in E. coli [12] and attributed to the interaction of water molecules with cellular components. The population of "slow" water molecules accounts for a much smaller fraction of the scattering signal (from 6% to 17% depending on the cell type) and characterized by smaller diffusion coefficient and longer residence times than those of bulk water. If the fractions of "fast" and "slow" intracellular water are defined as $F_{fast} = p_2/(p_1 + p_2)$ and

Irina Piazza, et al., Front. Phys. 13(1), 138301 (2018)

138301-5

Table 1 Parameter values obtained from the global fits.

	E. coli		Glioma-9L		Yeast	
	Value	Error	Value	Error	Value	Error
$f\%$	7.1	0.2	6.5	0.2	8.2	0.1
$p_1\%$	13.7	0.1	6.2	0.3	17.7	0.2
D_T^{slow} (cm^2/s)	2.1E-6	2E-7	3.9E-6	6E-7	2.2E-6	1E-7
τ_r^{slow} (ps)	34	2	53	12	33	2
D_R^{slow} (1/ps)	0.043	0.002	0.12	0.03	0.041	0.002
$p_2\%$	70.2	0.2	81.0	0.6	65.0	0.3
D_T^{fast} (cm^2/s)	2.13E-5	1E-7	2.16E-5	2E-7	2.04E-5	2E-7
τ_r^{fast} (ps)	1.28	0.02	0.84	0.06	1.65	0.04
D_R^{fast} (1/ps)	0.20	0.01	0.19	0.02	0.20	0.01
Γ_{CH_2} (meV)	0.170	0.01	0.118	0.002	0.273	0.003
$p_3\%$	9	0.2	6.3	1.2	9.1	0.6
χ_{rid}^2	1.58		0.54		1.01	

Table 2 Fractions of "fast" and "slow" water populations together with translational and rotational retardation factors for various biological samples. RBC: Red blood cells; Hmm: Haloarcula marismortui.

SAMPLE [Ref.]	F_{fast}	F_{slow}	R_{trasl}	R_{rot}	Exp. technique
RBC [9]	90%	10%	40		QENS
E. coli cells [10]	85%	15%		15	NMR
E. coli cells [7]	100%	0%			QENS
Hmm cells [7]	24%	76%	250		QENS
Hmm cells [10]	85%	15%		15	NMR
E. coli cells [this work]	85%	15%	10	5	QENS
Yeast cells [this work]	79%	21%	9	5	QENS
Glioma-9L cells [this work]	93%	7%	6	1.6	QENS
Bovine brain [18]	82%	18%	10	2.7	QENS

$F_{slow} = p_1/(p_1+p_2)$, and the translational and rotational retardation factors are denoted as $R_{trasl} = D_{fast}^T/D_{slow}^T$ and $R_{rot} = D_{fast}^R/D_{slow}^R$, our results can be compared on equal footing with the existing literature values of water in cells and in tissues. Such a comparison is shown in Table 2.

Data shown in Table 2 highlight one general feature that appears to be common to all biological systems investigated, specifically the presence of two intracellular water populations: a majority one having dynamic properties, i.e., translational and rotational diffusion coefficient and residence time, similar to bulk water and a minority one characterized by slow dynamics. This result is fully confirmed by our data. In this sense, we agree with the result by Jasnin *et al.* in 2010 [12] that intracellular water is not substantially "tamed" by confinement. However, the new information brought by our results is that the described extent of intracellular water perturbation, i.e., the fractions of "fast" and "slow" water populations, the retardation factors, the increase in residence times,

depends on cellular biodiversity, and applies not only to thermophilic organisms, but also to mesophilic ones. A clear example is given by the Glioma-9L tumoral cells, where the intracellular water appears to be more dynamic both for the water populations (F_{fast} is increased to 93% with F_{slow} reduced to 7%) and for retardation factors, with values reduced to 6 and 1.6 for translations and rotations, respectively. It is difficult to relate the increased dynamics of intracellular water to the carcinogenic or morphological properties of Glioma-9L cells; however, this new and motivating result prompts for further investigations in this field.

4 Conclusions

In this work, we have measured the QENS spectra of three different types of cells. To analyze the measured spectra, we have adopted a global fitting strategy, in which all spectra, taken at different Q values and at

two different energy resolutions are globally fitted using an optimized theoretical model that considers various classes of hydrogen atoms contributing to the scattering signal. In particular, we have been able to single out two different populations of intracellular water molecules and characterize their translational and rotational dynamic properties. Particular care has been taken to verify the validity of the model and to check the reliability of the calculation of parameters and their 99% confidence limit intervals. The main results obtained can be summarized as follows:

(i) The presence of two populations of intracellular water, a majority one with bulk-like dynamics and a minority one with slow dynamics, appears to be a general property of biological systems including living cells and tissues.

(ii) Cellular/tissutal biodiversity manifests itself in the extent of intracellular water retardation, both in the fast/slow water population fractions and in the retardation factors.

(iii) Therefore, neutron scattering appears to be a suitable experimental technique to characterize the dynamics of water inside living cells and tissues at the angstrom/picosecond space/time scales, and to investigate the effects of biodiversity.

References

1. P. Ball, Water as an active constituent in cell biology, *Chem. Rev.* 108(1), 74 (2008)

2. G. Schirò, F. Natali, and A. Cupane, Physical origin of anharmonic dynamics in proteins: New insights from resolution-dependent neutron scattering on homomeric polypeptides, *Phys. Rev. Lett.* 109(12), 128102 (2012)

3. G. Schirò, M. Fomina, and A. Cupane, Communication: Protein dynamical transition vs. liquid-liquid phase transition in protein hydration water, *J. Chem. Phys.* 139(12), 121102 (2013)

4. G. Zaccai, The effect of water on protein dynamics, *Philos. Trans. R. Soc. Lond. B Biol. Sci.* 359(1448), 1269 (2004)

5. G. Zaccai, Hydration shells with a pinch of salt, *Biopolymers* 99(4), 233 (2013)

6. E. Trantham, H. Rorschach, J. Clegg, C. Hazlewood, R. Nicklow, and N. Wakabayashi, Diffusive properties of water in Artemia cysts as determined from quasi-elastic neutron scattering spectra, *Biophys. J.* 45(5), 927 (1984)

7. M. Tehei, B. Franzetti, K. Wood, F. Gabel, E. Fabiani, M. Jasnin, M. Zamponi, D. Oesterhelt, G. Zaccai, M. Ginzburg, and B.Z. Ginzburg, Neutron scattering reveals extremely slow cell water in a Dead Sea organism, *Proc. Natl. Acad. Sci. USA* 104(3), 766 (2007)

8. M. Jasnin, A. Stadler, M. Tehei, and G. Zaccai, Specific cellular water dynamics observed in vivo by neutron scattering and NMR, *Phys. Chem. Chem. Phys.* 12(35), 10154 (2010)

9. A. M. Stadler, J. P. Embs, I. Digel, G. M. Artmann, T. Unruh, G. Buldt, and G. Zaccai, Cytoplasmic water and hydration layer dynamics in human red blood cells, *J. Am. Chem. Soc.* 130(50), 16852 (2008)

10. E. Persson and B. Halle, Cell water dynamics on multiple time scales, *Proc. Natl. Acad. Sci. USA* 105(17), 6266 (2008)

11. S. Moreno, A. Klar, and P. Nurse, Molecular genetic analysis of fission yeast Schizosaccharomyces pombe, *Methods Enzymol.* 194, 795 (1991)

12. M. Jasnin, M. Moulin, M. Haertlein, G. Zaccai, and M. Tehei, Down to atomic-scale intracellular water dynamics, *EMBO Rep.* 9(6), 543 (2008)

13. D. Richard, M. Ferrand, and G. Kearley, Analysis and visualisation of neutron-scattering data, *Journal of Neutron Research* 4(1), 33 (1996)

14. M. Bee, Quasielastic Neutron Scattering: Principles and Applications in Solid State Chemistry. Biology and Materials Science, Adam Hilger, Bristol, 1988

15. V. Sears, Theory of cold neutron scattering by homonuclear diatomic liquids (i): Free rotation, *Can. J. Phys.* 44(6), 1279 (1966)

16. J. Teixeira, M. C. Bellissent-Funel, S. H. Chen, and A. J. Dianoux, Experimental determination of the nature of diffusive motions of water molecules at low temperatures, *Phys. Rev. A* 31(3), 1913 (1985)

17. W. T. Vetterling, Numerical Recipes Example Book (C++): The Art of Scientific Computing, Cambridge University Press, 2002

18. F. Natali, Y. Gerelli, C. Stelletta, and J. Peters, Anomalous proton dynamics of water molecules in neural tissue as seen by quasi-elastic neutron scattering: Impact on medical imaging techniques, in: AIP Conference Proceedings, Vol. 1518 (AIP, 2013), pp 551–557

Irina Piazza, et al., Front. Phys. 13(1), 138301 (2018)

138301-7

Frontiers of Physics